Tensor-based characteristic impedance calculations of microstrips on ferrite-dielectric substrates for integrated phase shifter applications

Z. Cai
S. Xiao
J. Bornemann
R. Vahldieck

Indexing terms: Ferrites and ferromagnetics, Microstrip and stripline

Abstract: The influences of tensor parameters on the characteristics of microstrip structures on layered ferrite-dielectric substrates for phase shifter applications are investigated. By fully incorporating the permeability tensor into the numerical model, it is found that the propagation constant, and particularly the characteristic impedance values, are substantially lower than those commonly calculated under the scalar permeability assumption. The variation of the characteristic impedance is presented with respect to magnetisation levels, saturation magnetisations and the thickness of the ferrite layer.

1 Introduction

Printed circuit structures on ferrite substrates [1–3] are used in applications such as phase shifters [4], magnetic film isolators or circulators [6]. In particular, a composite microstrip structure involving a ferrite-dielectric layered substrate [4, 5] has been found suitable for phase shifter applications in microwave integrated circuits. For these structures, the accurate calculation of both dispersion behaviour and characteristic impedance is of fundamental importance.

Several analytical methods have been investigated considering reciprocal as well as nonreciprocal properties. However, the applied techniques are usually based on a quasi-static-approximation assuming a scalar permeability [6]. More rigorous tensor-based analyses, which only solve the propagation characteristics of ferrite-dielectric layered microstrip configurations, have been presented using the spectral domain approach [7, 12] or the method of lines [8]. Besides the fact that the computations [7] are restricted to narrowband calculations and a high-applied magnetic field, neither of these papers present data on, or even mention, the characteristic impedance, which is an extremely important factor, e.g. for low-reflection phase shifter design.

Therefore, this paper focuses on the characteristic impedance calculation of ferrite-dielectric layered microstrip lines. It is demonstrated that to obtain reliable data on the characteristic impedance, the scalar permeability assumption is not sufficient, but the full tensor needs to be considered. The applied theory is based on the spectral domain approach [9] and includes the magnetisation of the ferrite layer in propagation direction as well as the anisotropic effects of the permeability tensor. Therefore, an accurate numerical model for the calculation of both the normalised propagation constant and the characteristic impedance is obtained. In the example of an integrated circuit phase shifter structure, the influence of the tensor parameters are demonstrated with respect to different magnetisation levels, different saturation magnetisations and the thickness of the ferrite layer.

Paper 8625H (E12), received 28th August 1991

The authors are with the Laboratory for Lightwave Electronics, Microwaves and Communications, Department of Electrical and Computer Engineering, University of Victoria, PO Box 3055, Victoria, BC, Canada V8W 3P6

2 Theory

Fig. 1 shows the cross-section of the microstrip line under investigation and the co-ordinate system for the analysis.

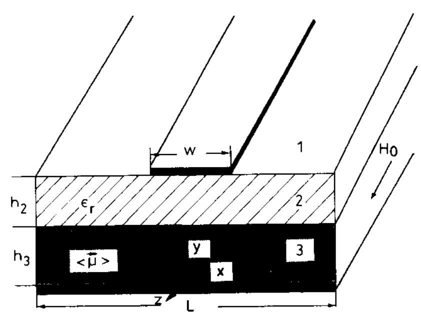

Fig. 1 *Cross-section of ferrite-dielectric-substrate microstrip line*

With the biasing DC magnetic field H_o in propagation direction [5], the permeability tensor reads

$$\langle \tilde{\mu} \rangle = \mu_0 \begin{pmatrix} \mu & -j\kappa & 0 \\ j\kappa & \mu & 0 \\ 0 & 0 & \mu_z \end{pmatrix} \tag{1}$$

where μ, κ and μ_z are real quantities. For the demagnetised ferrite, the relative permeability element [2] can be expressed as

$$\mu_{dem} = \frac{1}{3}\left\{1 + 2\sqrt{\left[1 - \left(\frac{\omega_m}{\omega}\right)^2\right]}\right\} \tag{2}$$

where

$$\omega_m = \gamma(4\pi M_s) \tag{3}$$

ω is the operating angular frequency, γ is the gyromagnetic ratio and $4\pi M_s$ is the saturation magnetisation.

In the general case of a partially magnetised ferrite, the experimental expressions for μ, κ and μ_z are used [5]

$$\mu = \mu_{dem} + (1 - \mu_{dem})(4\pi M/4\pi M_s)^{3/2} \tag{4}$$

$$\kappa = \frac{\gamma(4\pi M)}{\omega} \tag{5}$$

$$\mu_z = \mu_{dem}[1 - (4\pi M/4\pi M_s)]^{5/2} \tag{6}$$

The electromagnetic field in each homogeneous subregion $i = 1, 2$ and 3 (see Fig. 1)

$$\begin{aligned} \nabla \times \vec{H} &= j\omega\varepsilon\vec{E} \qquad \nabla(\langle\vec{\mu}\rangle\vec{H}) = 0 \\ \nabla \times \vec{E} &= -j\omega\langle\vec{\mu}\rangle\vec{H} \qquad \nabla\vec{E} = 0 \end{aligned} \tag{7}$$

is calculated from the E_z and H_z components. In regions $i = 1$ and 2, the Helmholtz equation

$$\frac{\partial^2}{\partial y^2}\begin{pmatrix}\tilde{E}_{zi}\\ \tilde{H}_{zi}\end{pmatrix} - k_i^2\begin{pmatrix}\tilde{E}_{zi}\\ \tilde{H}_{zi}\end{pmatrix} = 0 \tag{8}$$

is solved by

$$\begin{pmatrix}\tilde{E}_{z1}\\ \tilde{H}_{z1}\end{pmatrix} = \begin{pmatrix}A_1\\ B_1\end{pmatrix}\exp\{-k_1(y - h_2 - h_3)\} \tag{9}$$

$$\begin{pmatrix}\tilde{E}_{z2}\\ \tilde{H}_{z2}\end{pmatrix} = \begin{pmatrix}A_2\\ B_2\end{pmatrix}\sinh\{k_2(y - h_3)\} + \begin{pmatrix}C_2\\ D_2\end{pmatrix}\cosh\{k_2(y - h_3)\} \tag{10}$$

where the tilde denotes the Fourier transform, A_i to D_i are amplitude coefficients and $k_i^2 = \omega^2\varepsilon_0\varepsilon_{ri}\mu_0$ ($i = 1$, 2 and 3).

In region 3, the coupled Helmholtz equations derived from eqns. 1 and 7 read

$$\begin{aligned} \frac{\partial^2\tilde{E}_z}{\partial y^2} - k_e^2\tilde{E}_z &= g_e\tilde{H}_z \\ \frac{\partial^2\tilde{H}_z}{\partial y^2} - k_h^2\tilde{H}_z &= g_h\tilde{E}_z \end{aligned} \tag{11}$$

where

$$\begin{aligned} k_e^2 &= \beta^2 + \alpha_n^2 - k_3^2\mu_z\mu_e \\ k_h^2 &= \frac{\beta^2}{\mu} + \alpha_n^2 - k_3^2\mu_z \end{aligned} \tag{12}$$

$$g_e = \beta\kappa^2\mu_z/\mu \quad g_h = g_e\varepsilon_{r3}/\mu \tag{13}$$

$$\mu_e = \frac{\mu^2 - \kappa^2}{\mu} \quad \alpha_n = \frac{n\pi}{L} \tag{14}$$

The solutions of eqn. 11 can be expressed as

$$\tilde{E}_{z3} = A_3e^{-r_1y} + B_3e^{r_1y} - Z(C_3e^{-r_2y} + D_3e^{r_2y}) \tag{15}$$

$$\tilde{H}_{z3} = -Y(A_3e^{-r_1y} + B_3e^{r_1y}) + C_3e^{-r_2y} + D_3e^{r_2y} \tag{16}$$

with

$$Z = \frac{g_e}{r_2^2 - k_e^2} \quad Y = \frac{g_h}{k_h^2 - r_2^2}$$

$$r_{1,2}^2 = \frac{k_e^2 + k_h^2 \pm \sqrt{\{(k_e^2 - k_h^2)^2 + 4g_eg_h\}}}{2} \tag{17}$$

By matching the field components at interfaces h_3 and $h_3 + h_2$, and introducing the well known current distributions on the strip

$$\begin{aligned} \tilde{J}_{xi}(x) &= \frac{\sin\left\{i\pi\left(\frac{2x}{w} + 1\right)\right\}}{\sqrt{\left\{1 - \left(\frac{2x}{w}\right)^2\right\}}} \\ \tilde{J}_{zi}(x) &= \frac{\cos\left\{(i-1)\pi\left(\frac{2x}{w} + 1\right)\right\}}{\sqrt{\left\{1 - \left(\frac{2x}{w}\right)^2\right\}}} \end{aligned} \tag{18}$$

and applying the Galerkin method in the spectral domain [9, 10], the characteristic matrix equation system of the ferrite-dielectric layered microstrip structure can be formulated. After obtaining the propagation constant for the dominant mode as the first zero of the system determinant, the characteristic impedance defined as the ratio of power and current [11] can be calculated.

3 Results

In Figs. 2 and 3, the line characteristics obtained with this method are compared with those reported in the literature for integrated circuit phase shifter applications [5]. For a demagnetised ferrite layer, Fig. 2 demonstrates good agreement between the quasi-static-approximation [5] and this method using an effective permeability. By including the tensor properties, however, the analysis produces lower values for the normalised propagation-constant (Fig. 2*a*) and the characteristic impedance (Fig. 2*b*). This effect is even more pronounced towards higher frequencies.

A similar behaviour is observed in Figs. 3*a* and *b* for the polarised ferrite layer. It should be noted that the difference in characteristic impedance between the quasi-static-approximation [5] and the rigorous tensor-based method presented here is now slightly increased, compared with the demagnetised case in Fig. 2. This is due to the fact that the tensor parameters have a reduced influence on the guided wave effect, as opposed to the scalar permeability assumption. Therefore tensor components need to be considered in the accurate computer-aided design of integrated ferrite-dielectric phase shifter components as phase, and especially matching relations, are directly influenced by the propagation constant and characteristic impedance, respectively.

Figs. 4*a* and *b* show the line characteristics as a function of the magnetic bias with the saturation magnetisation as a parameter. The frequency is kept constant at 9 GHz. Both the propagation constant (see Fig. 4*a*) and the characteristic impedance (see Fig. 4*b*) decrease with magnetisation and increase with saturation magnetisation. Also, the difference in characteristic impedance between high and low-applied magnetisation becomes larger as the saturation magnetisation is reduced. This is due to the fact that the influence of the tensor parameters lead to a larger variation with increasing applied magnetic bias.

Fig. 5 demonstrates the range of variations in propagation constant and characteristic impedance with respect to the thickness of the ferrite layer. The increase in the normalised propagation constant towards thicker ferrite layers and the relatively small reduction in characteristic impedance is clearly a result of the layered structure and, in particular, the influence of the tensor parameters. As the power-current-defined characteristic impedance of a standard microstrip structure on a purely dielectric substrate shows opposite tendencies, this demonstrates again the necessity of tensor-based numerical models for the evaluation of microstrip impedance and propagation characteristics.

4 Conclusions

The influence of tensor parameters on the characteristic impedance and normalised propagation constant of ferrite-dielectric layered microstrip lines has been investigated. It has been found that by considering the permeability tensor, the characteristic impedance values are substantially lower than those obtained with the commonly used scalar permeability approximation. Line characteristics have been presented with respect to magnetisation levels, saturation magnetisations and the thick-

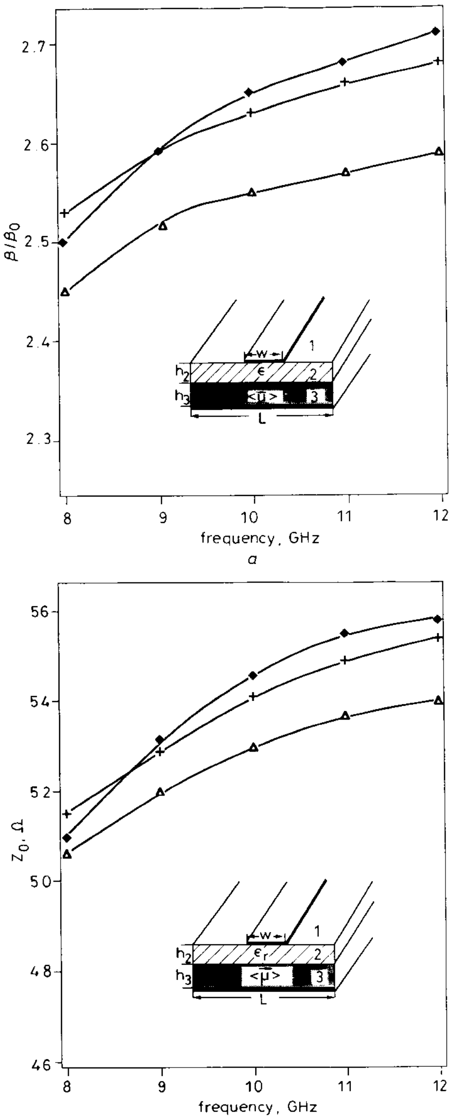

Fig. 2 *Comparison of this method with Reference 5 for demagnetised ferrite*

a Normalised propagation constant
b Characteristic impedance
Dimensions: $w = 0.67$ mm; $h_2 = 0.254$ mm; $h_3 = 0.8$ mm; $L = 20$ mm; $\varepsilon_{r2} = 9.9$; $\varepsilon_{r3} = 16.6$; $4\pi M_s = 2800$ Gauss
—◆— μ_{eff} [5]
—+— μ_{eff} (this method)
—Δ— $\langle\bar{\mu}\rangle$ (this method)

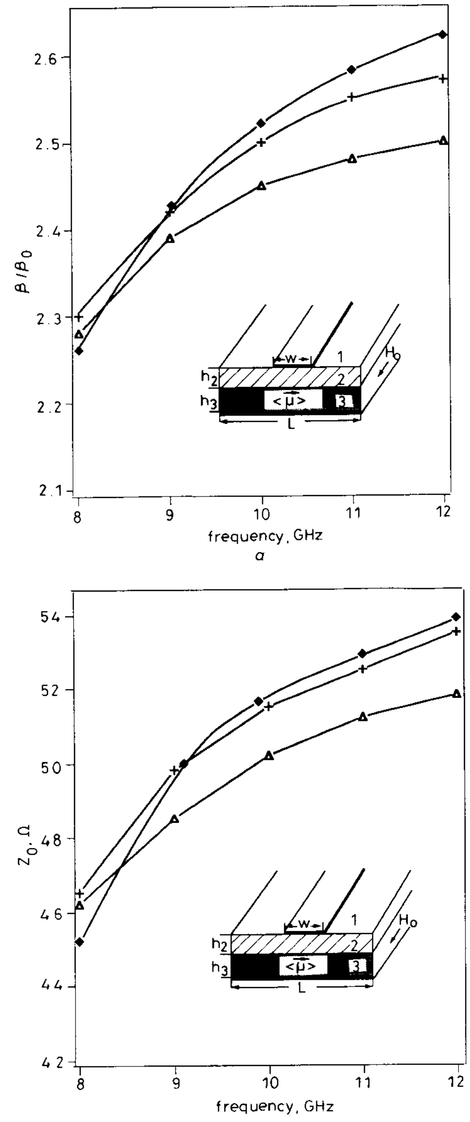

Fig. 3 *Comparison of this method with Reference 5 for polarised ferrite*

a Normalised propagation constant
b characteristic impedance
Dimensions according to Fig. 2; $w = 0.67$ mm; $h_2 = 0.254$ mm; $h_3 = 0.8$ mm; $L = 20$ mm; $\varepsilon_{r2} = 9.9$; $\varepsilon_{r3} = 16.6$; $4\pi M_{max} = 2240$ Gauss
—◆— μ_{eff} [5]
—+— μ_{eff} (this method)
—Δ— $\langle\bar{\mu}\rangle$ (this method)

ness of the ferrite layer. The results obtained for the characteristic impedance clearly demonstrate the necessity for tensor-based models in the computer-aided analysis and design of integrated microstrip circuits.

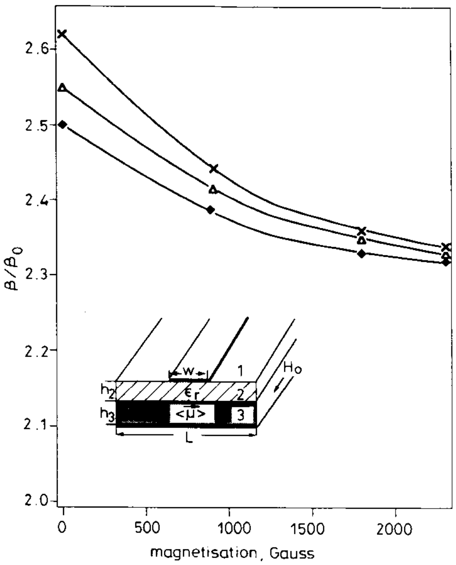

a

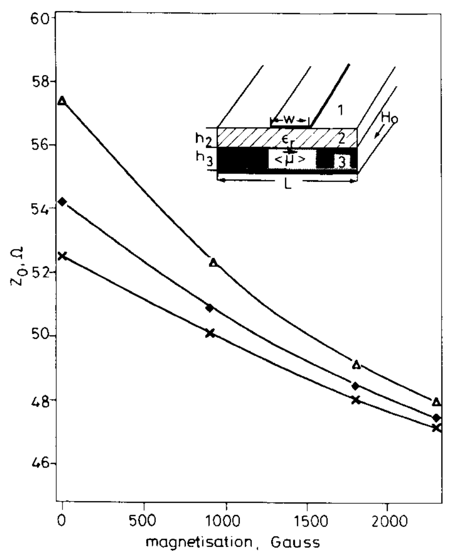

b

Fig. 4 *Normalised propagation constant and characteristic impedance against magnetisation*

$w = 0.67$ mm; $h_2 = 0.254$ mm; $h_3 = 0.8$ mm; $L = 20$ mm; $\epsilon_{r2} = 9.9$; $\epsilon_{r3} = 16.6$

a Normalised propagation constant

—◆— $4\pi M_s = 2800$ Gauss

—Δ— $4\pi M_s = 2700$ Gauss

—×— $4\pi M_s = 2500$ Gauss

b Characteristic impedance

—×— $4\pi M_s = 2800$ Gauss

—◆— $4\pi M_s = 2700$ Gauss

—Δ— $4\pi M_s = 2500$ Gauss

5 Acknowledgment

The authors would like to thank Dr. Ke Wu for his helpful discussions and suggestions.

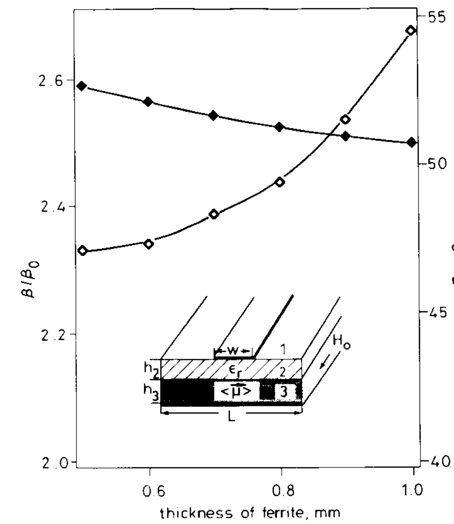

Fig. 5 *Normalised propagation constant and characteristic impedance against ferrite thickness*

$w = 0.67$ mm; $h_2 = 0.254$ mm; $h_3 = 0.8$ mm; $L = 20$ min; $\epsilon_{r2} = 9.9$; $\epsilon_{r3} = 16.6$

—◆— z_0

—Δ— β/β_0

6 References

1 HINES, M.E.: 'Reciprocal and nonreciprocal modes of propagation in ferrite stripline and microstrip devices', *IEEE Trans.*, 1971, **MTT-19**, pp. 442–451

2 PUCEL, R.A., and MASSE, D.J.: 'Microstrip propagation on magnetic substrates — Part II: Design theory', *IEEE Trans.*, 1972, **MTT-20**, pp. 304–308

3 HOFMANN, H.: 'Dispersion of the ferrite-filled microstrip-line', *AEU*, 1974, **28**, pp. 223–227

4 HANSSON, E.R.B., ADITYA, S., and LARSSON, M.A.: 'Planar meanderline ferrite-dielectric phase shifter', *IEEE Trans.*, 1981, **MTT-29**, pp. 209–215

5 BOLIOLI, S., BENZINA, H., BAUDRAND, H., and CHAN, B.: 'Centimeter-wave microstrip phase shifter on a ferrite-dielectric substrate', *IEEE Trans.*, 1989, **MTT-37**, pp. 698–705

6 WEBB, D.C.: 'Microwave magnetic thin-film devices', *IEEE Trans. Magn.*, 1988, **24**, pp. 2799–2804

7 TSUTSUMIAND, M., and ASAHARA, T.: 'Microstrip lines using yttrium iron garnet film', *IEEE Trans.*, 1990, **MTT-38**, pp. 1461–1467

8 PREGLA, R., and WORM, S.B.: 'The method of lines for the analysis of planar waveguides with magnetized ferrite substrate'. 1984 IEEE MTT-S Int. Microwave Symp. Dig., 1984, pp. 348–350

9 ITOH, T., and HEBERT, A.S.: 'A generalized spectral domain analysis for coupled suspended microstrip lines with tuning septums', *IEEE Trans.*, 1978, **MTT-26**, pp. 820–826

10 GESHIRO, M., and ITOH, T.: 'Analysis of double-layered finlines containing a magnetized ferrite', *IEEE Trans.*, 1987, **MTT-35**, pp. 1377–1381

11 DENLINGER, E.J.: 'A frequency dependant solution for microstrip transmission lines', *IEEE Trans.*, 1971, **MTT-19**, pp. 30–39

12 KITAZAWA, T.: 'Analysis of shielded striplines and finlines with finite metallization thickness containing magnetized ferrites', *IEEE Trans.*, 1991, **MTT-39**, pp. 70–74